INTERFACE

Raman spectroscopy and CARS imaging: prospective tools for monitoring skeletal cells and skeletal regeneration

Journal:	Journal of the Royal Society Interface	
Manuscript ID	rsif-2016-0182.R1	
Article Type:	Review	
Date Submitted by the Author:	n/a	
Complete List of Authors:	Moura, Catarina; University of Southampton Tare, Rahul; University of Southampton Oreffo, Richard; University of Southampton, Bone and Joint Research Group Mahajan, Sumeet; University of Southampton,	
Categories:	Life Sciences - Physics interface	
Subject:	Chemical biology < CROSS-DISCIPLINARY SCIENCES, Medical physics < CROSS-DISCIPLINARY SCIENCES	
Keywords:	CARS, Raman spectroscopy, Coherent Raman, skeletal, stem cells	

SCHOLARONE™ Manuscripts Title:

Raman spectroscopy and CARS imaging: prospective tools for monitoring skeletal cells and skeletal regeneration

Authors:

Catarina Costa Moura ^{a, b}
Rahul S. Tare ^b
Richard O. C. Oreffo ^b
Sumeet Mahajan ^a

^a Department of Chemistry and Institute for Life Sciences, Highfield Campus, University of Southampton, SO17 1BJ.

^b Bone and Joint Research Group, Centre for Human Development, Stem Cells and Regeneration, Institute of Developmental Sciences, University of Southampton, SO16 6YD, UK.

Abstract:

The use of skeletal stem cells (SSCs) for cell-based therapies is currently one of the most promising areas for skeletal disease treatment and skeletal tissue repair. The ability for controlled modification of SSCs could provide significant therapeutic potential in regenerative medicine, with the prospect to permanently repopulate a host with stem cells and their progeny. Currently, SSC differentiation into the stromal lineages of bone, fat and cartilage is assessed using different approaches that typically require cell fixation or lysis, which are invasive or even destructive. Raman spectroscopy and coherent anti-Stokes Raman scattering (CARS) microscopy present an exciting alternative for studying biological systems in their natural state, without any perturbation. Here we review the applications of Raman spectroscopy and CARS imaging in stem cell research, and discuss the potential of these two techniques for evaluating SSCs, skeletal tissues and skeletal regeneration as an exemplar.

Keywords: CARS, coherent, Raman, skeletal, stem cells

Introduction:

Throughout the last century, medical breakthroughs have led to a tremendous increase in life expectancy. However, as a consequence, an increasing aging population has resulted in an increase in agerelated diseases, as well as associated reductions in quality of life, leading to a dramatic impact on healthcare. Indeed, skeletal tissue loss due to injury or disease results in significantly reduced quality of life at significant socio-economic cost. Fractures alone cost the European economy €17 billion and the US economy \$20 billion annually [1]. In the US, there are around 8 million bone fractures per year, of which approximately 5% to 10% are associated with delayed healing or non-union [2]. Each year in the UK there are approximately 150,000 wrist, vertebral and hip fractures due to osteoporosis, with an estimated healthcare cost of £2.1 billion per annum. Thus, novel and effective medical approaches are essential to fulfil the current demographic challenges [3-5].

The use of stem cells for cell-based therapies is one of the most promising and exciting areas for tissue repair and disease treatment, including those affecting brain, skeletal muscle, and heart [6, 7]. In fact, the unique properties of stem cells, with their ability to self-renew and potential to differentiate into several different specialised cell types, present an ideal tool for reparative medicine [3, 8].

The bone marrow, which is the major site of haematopoiesis (the process which leads to the formation of all blood cells), serves as a reservoir for a variety of cells, including haematopoietic cells as well as cells of the non-haematopoietic stroma [4, 9-11]. The bone marrow stroma constitutes the scaffold that supports the regulation of haematopoiesis, establishing and maintaining the haematopoietic microenvironment necessary for growth and blood cell maturation [9, 12]. Within the bone marrow stroma reside a rare multipotent stem cell population called skeletal stem cells (SSCs). The term "skeletal stem cell" is all too frequently confused with "mesenchymal stem cell" (MSC) in the literature (reviewed in Bianco and Robey 2015 [12]). However, MSCs are developmentally distinct from skeletal lineages, and it is important to recognise that the various extraskeletal tissues and organs noted to retain MSCs are developmentally distinct from skeletal lineages and, critically, are not generated by skeletal progenitors present in bone marrow. The term "skeletal stem cell", as eloquently detailed by Bianco and Robey [13], denotes specifically the rare population of postnatal non-haematopoietic stromal cells found in the bone marrow with the capacity to regenerate bone and bone marrow stroma (reviewed in Dawson *et al.* 2014 [3]), and the term SSC will be used throughout this review to refer to this select population.

The ability to isolate SSCs from human bone marrow, together with their capability to differentiate into skeletal tissues, has attracted significant attention within the medical community, and promises new opportunities for the use of SSCs in clinical applications [3, 10, 14]. For example, SSCs could be applied for bone/cartilage tissue reparation for a range of musculoskeletal conditions, or as key components of the haematopoietic microenvironment for microvessel assembly guidance, or even as conceptual/modelling instruments for stem cell biology and mechanistic studies [12]. However, pivotal in the development of successful therapies for bone augmentation will be the design of well-defined and reproducible protocols for SSC differentiation. SSCs can be induced to form bone, cartilage, and fat depending on their microenvironment (Figure 1) [4, 15, 16], and the differentiation into osteoblasts, chondrocytes, and adipocytes,

both *in vitro* and *in vivo*, is plastic (reversible) [11]. Controlled differentiation of stem cells offers significant therapeutic potential in skeletal regeneration, with the prospective to permanently repopulate a host with stem cells and their progeny, an objective that could be achieved by careful monitoring and characterisation of the differentiation process of SSCs.

Currently SSC differentiation can be evaluated through a number of assays including colorimetric assays [17], real-time quantitative polymerase chain reaction (qPCR) [17, 18], histochemical analysis [18], and immunohistochemical assays [19]. These methods reveal the detailed biochemical features of SSCs and provide important information regarding their state of differentiation. However, current approaches are invasive, require cell fixation or lysis, and/or are destructive [20-22], indicating current monitoring techniques are unsuitable for time-course studies, as well as unsuitable for SSC characterisation prior to therapeutic use. For example, photobleaching of fluorophores/fluorescent dyes limits the temporal availability for imaging the sample of interest. A further important issue is the non-specific binding of dyes or labels, and the staining process may modify the functionality of the target molecule and affect cell biochemical phenomena [21, 23].

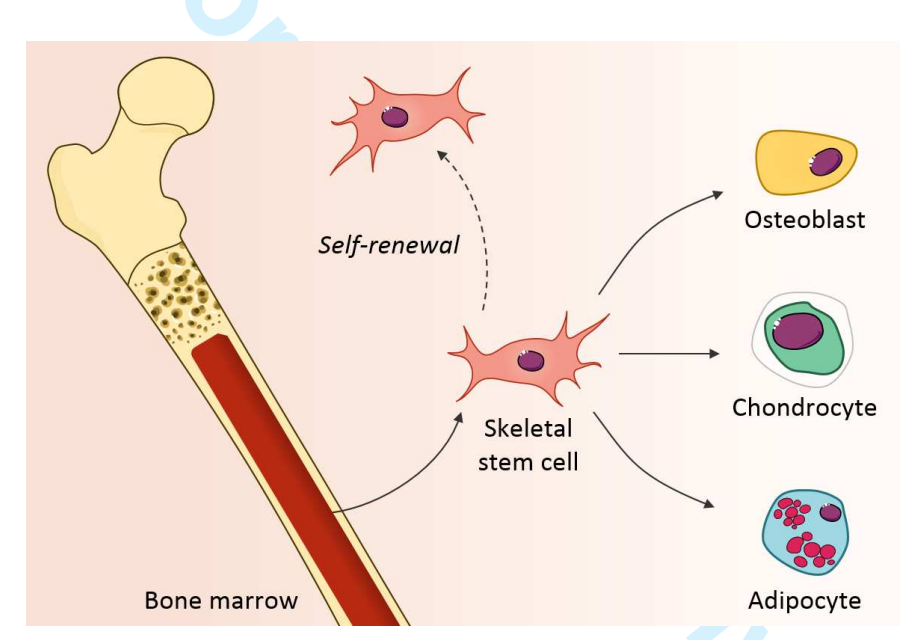


Figure 1 The differentiation potential of skeletal stem cells. A population of skeletal stem cells can be isolated and enriched from the human bone marrow, and expanded *in vitro*. Under appropriate conditions these skeletal stem cells have the ability to self-renew and to differentiate towards bone, cartilage and fat lineages.

The current limitations in the characterisation of SSC differentiation have led to the need to find new alternatives. Prospective approaches seek to identify molecules at sub-cellular level without using any dye or label, *i.e.* "label-free", but by using the intrinsic properties of the molecules. Label-free techniques which offer chemical or molecular selectivity are particularly attractive. Methods which rely on the measurement of vibrational information such as Raman spectroscopy and coherent anti-Stokes Raman scattering (CARS) microscopy are inherently non-invasive (as no introduction of labels is required), non-destructive, as well as chemically selective. It is noted that as with all optical techniques power and exposure to light need to be within a threshold to prevent any damage and phototoxic effects on cells. In this review, we present a detailed

overview of the recent applications of Raman spectroscopy and CARS microscopy in stem cell research, and discuss the potential of label-free techniques to study skeletal stem cells for skeletal regeneration.

Characterisation of skeletal stem cells using label-free approaches

Raman spectroscopy provides information from the intrinsic vibrations of molecules in their native state, without the need for an exogenous label [24-26], and has been explored as a label-free method for biological and biomedical applications. Fourier transform infrared (FTIR) spectroscopy, a technique which provides complementary information to Raman spectroscopy, has also been applied to biological samples in order to study their vibrational profile. However, FTIR is not ideal for biomedical imaging because water strongly absorbs infrared light [21, 23, 27]. Raman spectroscopy is typically carried out with visible or near infrared laser sources, and is ideal for measurement of biological samples in the natural state, as water is a very poor Raman scatterer. Both FTIR and Raman spectra can reveal a molecular fingerprint of SSCs, from single molecules to complex structures, providing broad chemical information on their content (lipids, proteins, nucleic acids, *et cetera*). A comparison of the key features from different characterisation methods for SSCs is presented in Table 1 [23, 25, 28-31], and it is possible to see that Raman spectroscopy and CARS microscopy offer some advantages over traditional SSC characterisation techniques.

Table 1 Comparison of the main features of skeletal stem cell characterisation techniques.

	Detection sensitivity	Quantitative analysis	Molecular specificity	Sample preparation	Non-invasive analysis	Time- consumption	<i>In vivo</i> relevance
Biochemical assays	Low	Semi	Medium	Yes	No	Medium	Medium
Histological assays	Low	No	Medium	Yes	No	High	High
qPCR	High	Yes	High	Yes	No	High	Low
IR spectroscopy	Medium	Yes	High	Yes	Yes	Low	Low
Raman spectroscopy	Low	Yes	High	No	Yes	Low	High
CARS	Medium	Semi	Medium	No	Yes	Low	High

Raman spectroscopy

When a beam of light interacts with a molecule, the energy is mostly scattered elastically (no change in energy) with the same frequency as the incident light, known as Rayleigh scattering (Figure 2a). A few incident photons interact and exchange energy with the molecular bond vibration, resulting in inelastically scattered light, also known as Raman scattering [31]. A molecule that absorbs a photon enters into a virtual excited state and, almost immediately, another photon is emitted at a slightly different wavelength. When the incident photon loses energy to a molecular bond vibration a red-shifted Stokes photon, *i.e.* a photon with longer wavelength, is generated and the molecule ends up in a higher vibrational state (Figure 2b). A blue-shifted anti-Stokes scattering can also occur, if the molecule of interest is already in a higher vibrational state,

resulting in the emission of a lower wavelength photon (Figure 2c). The difference in frequency between incident and scattered photons corresponds to the vibrational energy level of the molecule [23, 31-33], and is typically called Raman shift (since the shift in wavelength from the incident radiation is measured).

Since each molecule is unique with its own set of characteristic bonds and therefore vibrational modes, Raman spectroscopy provides a molecular "fingerprint". Given that cells and tissues are composed of different molecules, Raman spectroscopy offers, potentially, a powerful tool to generate a characteristic signature of SSCs and skeletal tissues.

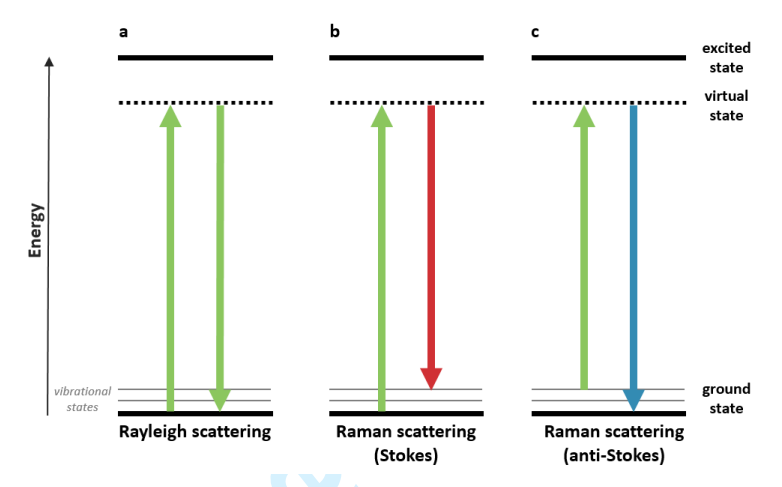


Figure 2 Schematic diagram of the energy transitions involved in Rayleigh scattering (a) and Raman scattering (b and c). Raman scattering occurs through the interaction of an incident photon with a molecular vibration mode, gaining (anti-Stokes scattering, blue-shifted) or losing (Stokes scattering, red-shifted) an amount of energy equal to that vibrational mode.

Furthermore, Raman spectroscopy offers other advantages to study living cells including: i) high spatial resolution, ii) qualitative and quantitative spectral information, iii) ability to detect at the subcellular level, and iv) the ability to analyse cells in real time without altering cell function, as a laser operating at the visible/near-infrared region is applied to prevent significant damage to proteins, DNA, RNA, and other present biomolecules [30, 34-37].

The last decade has witnessed the use of Raman spectroscopy in the search for prospective spectral markers for characterising stem cells, including murine embryonic stem cells [20, 37-39], human embryonic stem cells [21, 40-43], MSCs [21, 26, 35], SSCs [36, 44, 45], adipose-derived stem cells (ADSCs) [21, 46], as well as the monitoring of stem cell differentiation into skeletal tissues [21, 35, 36, 45, 46]. Table 2 summarises the current applications of Raman spectroscopy for stem cell research and the major outcomes. We discuss in detail those studies relevant for skeletal regeneration.

In 2009, Chiang *et al.* studied osteogenic differentiation of MSCs applying Raman spectroscopy, with the purpose to monitor the production of hydroxyapatite throughout the osteogenic process [35]. Chiang and colleagues found changes in the hydroxyapatite characteristic "chemical" shift, over the period of 7-21 days following the commencement of differentiation. The state of differentiation of MSCs was confirmed by the use of alizarin red S staining for calcium. Chiang *et al.* also detailed a novel marker in mesenchymal stem cell-derived osteoblasts by monitoring hydroxyapatite with Raman spectroscopy, providing the first indication that this technique could be a promising tool for the study of skeletal tissue development. Downes *et al.* also

induced MSC osteogenic differentiation for 7 days, and observed characteristic peaks in the osteoblasts spectra relating to phosphate in hydroxyapatite, collagen, and carbonate [21].

Similar approaches were used, where SSCs derived from human bone marrow, and subsequent differentiation into osteoblasts, were characterised and monitored [36, 45]. For example, McManus *et al.* used Raman spectroscopy as a biochemical characterisation tool for SSC differentiation into osteoblasts, and compared the results with immunocytochemistry and qPCR analysis (Figure 3) [45]. McManus *et al.* determined carbonate-to-phosphate and mineral-to-matrix ratios using specific peaks in Raman spectra at different stages of osteogenic development, and observed an increase of the two ratios with time. Hung's research group identified new spectral markers for osteogenic differentiation in SSCs [36]. In this case, the characteristic chemical shift of octacalcium phosphate was present before differentiation, and the peak decreased throughout the assay period. In contrast, the hydroxyapatite signal increased during SSCs differentiation into osteoblasts, and, in addition, a new peak belonging to the β-tricalcium phosphate appeared following differentiation. Hung *et al.* further corroborated their results using histochemical and gene expression analyses.

Other groups have reported on ADSCs for skeletal regeneration and their characterisation by Raman spectroscopy [21, 46]. Downes *et al.* differentiated ADSCs into osteoblasts and adipocytes, and characterised the different populations using Raman spectroscopy [47]. Similar to Hung's work [36], Ojansivu *et al.* recently used octacalcium phosphate, hydroxyapatite and β-tricalcium phosphate as specific markers for osteogenic differentiation, in order to compare culture conditions of ADSCs with different bioactive glasses [46]. More recently, Mitchell *et al.* demonstrated that Raman spectroscopy can be used to detect biochemical changes associated with adipogenic differentiation of ADSCs in a non-invasive and aseptic manner [48]. Mitchell and colleagues were able to monitor the adipogenic differentiation of live ADSCs during 14 days, and found significant differences from day 7.

An interesting possible application of Raman spectroscopy in SSC research, is the identification of different single-cell-derived clones, which could guide the search for new strategies to analyse the differentiation potential of SSCs, or even SSC isolation from human bone marrow. James *et al.* studied distinct subtypes of human bone marrow stromal cells, and Raman spectroscopy was applied to identify the molecular fingerprint of the stromal cells subtypes together with the biomolecular profile of human bone marrow CD317⁺ fractions [44]. Peak intensity ratios were obtained, and the main difference in the Raman shift was found at 1088.6 cm⁻¹, which is related to the symmetric phosphate stretch of the DNA backbone, indicating a fundamental difference in the DNA of the stromal cell subtypes.

Raman spectroscopic analysis is frequently applied in conjunction with multivariate statistical analysis, for example principal component analysis (PCA) and hierarchical clustering analysis (HCA) [26, 37, 45], due to the huge amount of chemical information embedded in Raman spectra. These methods provide an approach and are often necessary to extract information on different constituents which exist in varying proportions in a heterogeneous sample such as bone. In addition, a large amount of spectral data can be generated from a tissue map or from different populations (healthy *vs* diseased etc.). Identification of compositional changes, classification and quantification of concentrations requires the use of such statistical methods as has been shown in several studies with stem cells [40, 42, 45], and other diseases such as cancer [49]. Indeed, multivariate statistical methods for spectra analysis have contributed to the increase in

Raman spectroscopy applications in the examination of living cells, and could be a helpful and vital tool for the comparison of biological samples.

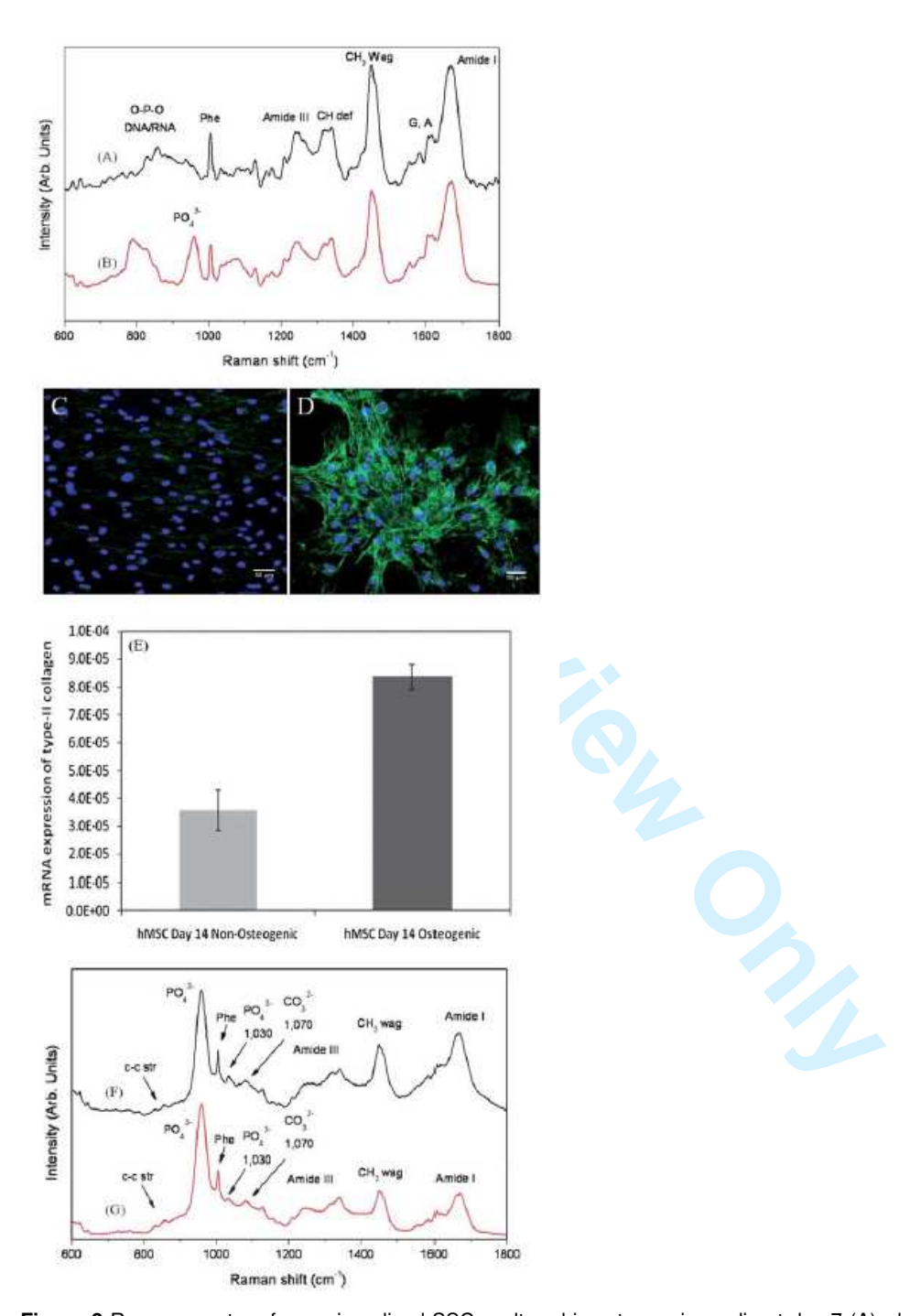


Figure 3 Raman spectra of pre-mineralised SSCs cultured in osteogenic media at day 7 (A), day 14 (B), day 21 (F) and day 28 (G). Immunocytochemical localisation of type II collagen in SSCs cultured for 14 days in basal media (C) and osteogenic media (D). Relative expression of type II collagen gene in SSCs cultured for 14 days in basal/osteogenic media, determined by qPCR (E). Adapted from [45]. Copyright Royal Society of Chemistry. Reproduced with permission.

Table 2 Raman spectroscopy applications in stem cells.

Reference (year)	Cell type	Study	Main findings
Notingher <i>et al.</i> (2004) [37, 39, 50]	Murine embryonic stem cells	Characterisation of murine embryonic stem cells	Changes in the Raman spectra in the RNA peak region can be used as a differentiation marker
Ichimura <i>et al.</i> (2014) [38]	Murine embryonic stem cells	Spontaneous differentiation of embryonic stem cells	Differences between Raman spectra of embryonic stem cells before and after spontaneous differentiation
Downes <i>et al.</i> (2011) [21]	Human embryonic stem cells	Characterisation of human embryonic stem cells	Differences in the Raman spectra between nucleus (higher levels of RNA) and cytoplasm (higher levels of protein and glycogen)
Chan <i>et al.</i> (2009) [40]	Human embryonic stem cells	Embryonic stem cell differentiation into cardiomyocytes	Changes in the RNA and DNA Raman peaks, before and after differentiation
Schulze <i>et al.</i> (2010) [42]	Human embryonic stem cells	Differentiation status of human embryonic stem cells	Identification of Raman bands and ratios (e.g. RNA/proteins) to indicate embryonic stem cell state of differentiation
Pascut <i>et al.</i> (2013) [41]	Human embryonic stem cells	Embryonic stem cell differentiation into cardiomyocytes	Changes in the Raman spectra of carbohydrates and lipids chemical shifts, increasing during differentiation process
Tan <i>et al.</i> (2012) [43]	Human embryonic stem cells & Human induced pluripotent stem cells	Differences between embryonic stem cells and induced pluripotent stem cells	Very similar Raman spectra, with small changes in the glycogen bands
Pijanka <i>et al.</i> (2010) [26]	Human embryonic stem cells & Human mesenchymal stem cells	Differences between human embryonic stem cells and MSCs	Raman scattering allowed to distinguish an increase in the DNA band when comparing the embryonic stem cells with the MSCs nuclei
Chiang <i>et al.</i> (2009)	Human mesenchymal stem cells	MSC differentiation into osteoblasts	Changes in the Raman spectra in the hydroxyapatite characteristic peak region during the osteogenic differentiation
Downes <i>et al.</i> (2011) [21]	Human mesenchymal stem cells	MSC differentiation into osteoblasts	Changes in the Raman spectra in the hydroxyapatite, collagen and carbonate chemical shifts during the osteogenic differentiation

McManus <i>et al.</i> (2011) [45]	Human skeletal stem cells	SSC differentiation into osteoblasts	Changes in the spectra in the hydroxyapatite Raman shift during osteogenic differentiation; Measurement of carbonate-to-phosphate and mineral-to-matrix ratios at different stages of development
Hung <i>et al.</i> (2013) [36]	Human skeletal stem cells	SSC differentiation into osteoblasts	Changes in the spectra in the octacalcium phosphate, β-tricalcium phosphate and hydroxyapatite Raman shifts, able to detect the extent of maturation during osteogenic differentiation
James <i>et al.</i> (2015) [44]	Human skeletal stem cells	Analysis of functional markers in SSCs using immortalised SSC clonal lines	Different SSC clones were identified by Raman spectroscopy, presenting the same bio-molecular profile as human SSC fractions
Downes <i>et al.</i> (2011) [21]	Human adipose-derived stem cells	ADSC differentiation into osteoblasts and adipocytes	Changes in the Raman spectra in the hydroxyapatite, collagen and carbonate chemical shifts after osteogenic differentiation; Raman peaks from lipids/proteins are sharper after adipogenic differentiation
Ojansivu <i>et al.</i> (2015) [46]	Human adipose-derived stem cells	ADSC differentiation into osteoblasts, using different bioactive glasses	Similarities in the hydroxyapatite, octacalcium and β-tricalcium phosphate Raman chemical shifts between different cell culture conditions
Mitchell <i>et al.</i> (2015) [48]	Human adipose-derived stem cells	ADSC differentiation into adipocytes	Characterisation of ADSC differentiation into adipocytes at early stages of differentiation

CARS imaging

While extremely powerful in terms of characterisation ability, the efficiency of Raman scattering is extremely small (approximately 1 in 10⁷ scattered photons [51]). Thus for imaging Raman scattering is rather limited as acquisition times per pixel can be up to several seconds. The use of alternative Raman-based techniques that can significantly boost and enhance Raman signal levels, such as coherent anti-Stokes Raman scattering (CARS) or surface-enhanced Raman scattering (SERS), offer exciting alternatives. SERS is highly sensitive but involves using an exogenous material to facilitate the read-out, usually functionalised metal nanoparticles, which may not be desirable. CARS provides the same label-free chemical contrast as Raman spectroscopy, although, and importantly from the current perspective, with improved sensitivity [52].

Coherent anti-Stokes Raman scattering occurs when a target molecule is irradiated using two laser beams simultaneously at different frequencies, a pump beam ω_P , and a Stokes beam ω_S (Figure 4) [53]. In essence, when the difference between the higher frequency (pump beam) and the lower frequency (Stokes beam) equals the vibrational frequency of the target bond of the molecule, a CARS signal is generated [32, 33, 52, 54], with an angular frequency equal to $\omega_{CARS} = 2\omega_P - \omega_S$. By tuning the frequencies of the two beams to match a particular vibration, a coherent signal with much higher intensity than the signal from spontaneous Raman scattering (up to five orders of magnitude [21, 55]) is emitted, providing a vibrational contrast in the subsequent CARS image [32, 52]. Acquisition times per pixel in CARS imaging are typically between 1 and 10 μ s.

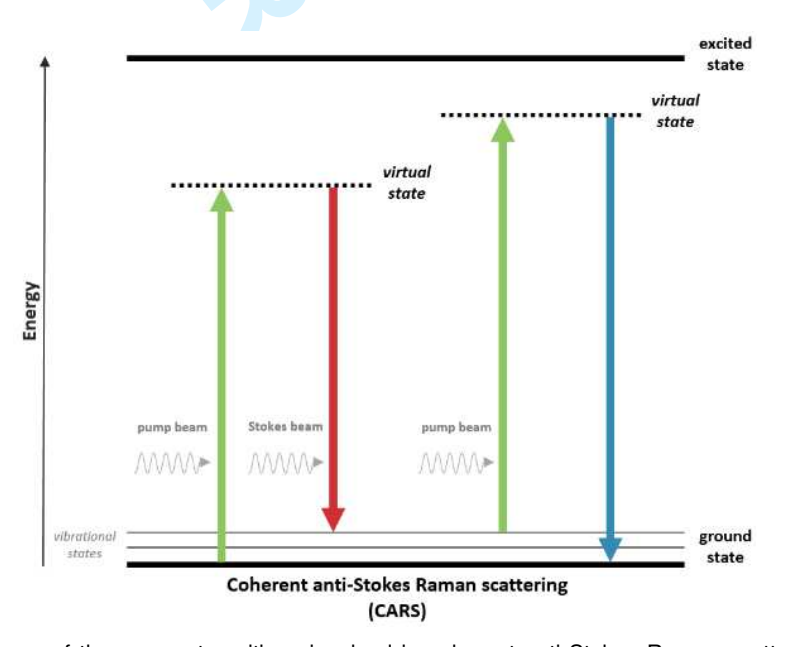


Figure 4 Schematic diagram of the energy transitions involved in coherent anti-Stokes Raman scattering (CARS). In CARS, molecular vibrational modes are coherently populated through optical pumping, by the combination of the pump and the Stokes. The vibrations coherence is probed by the pump to generate the CARS signal. Thus when the energy difference between the pump beam (higher frequency) and the Stokes beam (lower frequency) equals a particular molecular vibration of the target, the CARS signal is maximised.

CARS is a multiphoton (4-wave mixing) process with no net deposition of energy within the molecule (as illustrated in Figure 4), and is most often carried out with near infrared laser sources. Besides being non-invasive, non-destructive and label-free, CARS provides relevant benefits over other imaging techniques: i) the sample

photo-damage is minimised, since no net energy is transferred to the sample [54], ii) CARS provides inherent three-dimensional sectioning ability and video-rate imaging [23, 54, 56, 57], due to the non-linear multiphoton nature of CARS process, which is of paramount importance for studying cells or tissues, and iii) fluorescence does not interfere in CARS signal, as anti-Stokes Raman scattering occurs at a different (blue-shifted) wavelength from fluorescence [32, 52].

CARS microscopy has been applied in the imaging of living cells and *ex vivo* tissues, using diverse vibrational contrasts such as for DNA, lipids and proteins [10, 52, 54, 58]. Figure 5, as an example, shows the CARS imaging of a human squamous-cell carcinoma metastasis in the brain. Meyer *et al.* analysed the same tissue sample with CARS microscopy (targeting lipids) without any staining, and with brightfield microscopy after staining the sample with the gold standard haematoxylin and eosin (H&E).

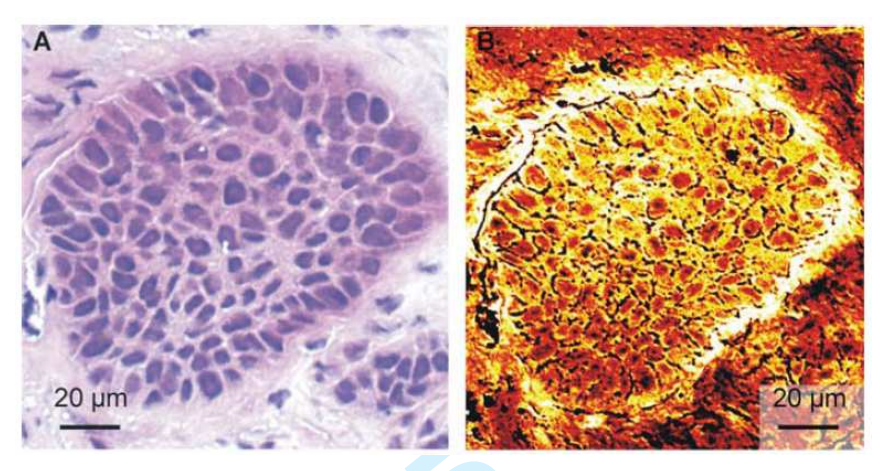


Figure 5 Comparison of H&E staining (A) and CARS imaging (B) of a human squamous-cell carcinoma metastasis in the brain. The bright components indicate the intensity of the CARS signal from lipids. Adapted from [59]. Copyright Wiley-VCH Verlag GmbH & Co. KGaA. Reproduced with permission.

The abundance and the essential role of lipids in the human body, combined with the fact that lipids have strong CH₂ and CH₃ stretching vibration signals at 2853 cm⁻¹ and 2935 cm⁻¹ [24, 52, 57], respectively, has made lipids the target of choice for demonstrating CARS applications. CARS applications in cell studies are being expanded – for instance, in order to develop an adipose-tumour epithelial cell co-culture system designed to reproduce the *in vivo* mammary environment, Salameh *et al.* required a non-destructive and non-invasive technique to access the viability of adipocytes in co-culture [60]. In this study, CARS analysis demonstrated the sustained viability of adipocytes, and an *ex vivo* co-culture model system to evaluate stromal-epithelial interactions in breast cancer was established. Another example is the application of CARS to study the effect of chemotherapeutic drugs in colon tumour cells. As demonstrated by Steuwe *et al.*, CARS was a useful tool to rapidly image the sub-cellular accumulation of lipids in cancer cells undergoing cell death induced by different chemotherapeutic drugs [24].

The last few years have seen emergent data of *in vitro* cell studies for skeletal regeneration that have applied CARS imaging. The principal findings regarding CARS applications for stem cell characterisation are summarised in Table 3. One of the first examples, shown in 2007 by Konorov *et al.*, used CARS microscopy to analyse murine embryonic stem cells [56]. Although image quality did not allow the identification of individual cells,

this approach provided a first step towards the use of CARS imaging in stem cell research. The following year, Schie *et al.* induced and characterised MSC differentiation into adipocytes, which is commonly assessed by identifying the development of lipid droplets. As the CARS signal for lipids is particularly strong, Schie and colleagues successfully imaged the lipid droplets after 21 days of adipogenic differentiation [61]. Recently, Smus *et al.* used CARS imaging to assess adipogenic differentiation of SSCs [62], in conjunction with molecular analysis of gene expression and conventional Oil Red O staining methodology. The authors demonstrated that CARS microscopy was a valuable technique to detect early stages of SSC differentiation (24 hours and 72 hours after adipogenesis induction), with enhanced resolution and definition of lipid droplets. Furthermore, CARS microscopy provided an alternative method to monitor changes in SSCs as a result of chemical modulation of adipogenic differentiation.

Different research groups have worked with ADSCs and monitored cell differentiation with CARS microscopy. Jo *et al.* selectively imaged lipid droplets with high contrast in differentiated adipocytes, and it was possible to observe a chronological differentiation of ADSCs, comparing Oil red O staining with CARS images [63]. In turn, Downes *et al.* not only used CARS microscopy to characterise adipocytes, but also tried to establish the use of CARS to image osteoblasts [21]. By imaging at the Raman frequency of hydroxyapatite (960 cm⁻¹), Downes obtained preliminary results with some vibrational contrast although with limited resolution.

Undoubtedly CARS imaging has emerged as an important alternative technique for monitoring the development of lipid droplets in SSCs. The combination of CARS microscopy with complementary imaging techniques, namely two-photon excitation fluorescence (TPEF) and second harmonic generation (SHG), can be highly advantageous and give an important insight on the development of SSCs from different angles. TPEF and SHG are also non-linear imaging modalities which usually can be carried out with the same laser excitation sources thus allowing multimodal readout. While TPEF allows mapping fluorophores (or auto-fluorophores) with near infrared excitation, SHG is particularly sensitive to non-centrosymmetric structures such as collagen. CARS together with SHG and/or TPEF could give a more holistic insight into the development of SSCs. Figure 6 shows an exciting application of CARS and SHG microscopy in our research group to assess the state of differentiation of foetal femur-derived SSCs. Simultaneous imaging of lipids (CARS) and collagen fibres (SHG) in human foetal femur-derived SSCs cultured in adipogenic (Figure 6a) and chondrogenic (Figure 6b) media is shown.

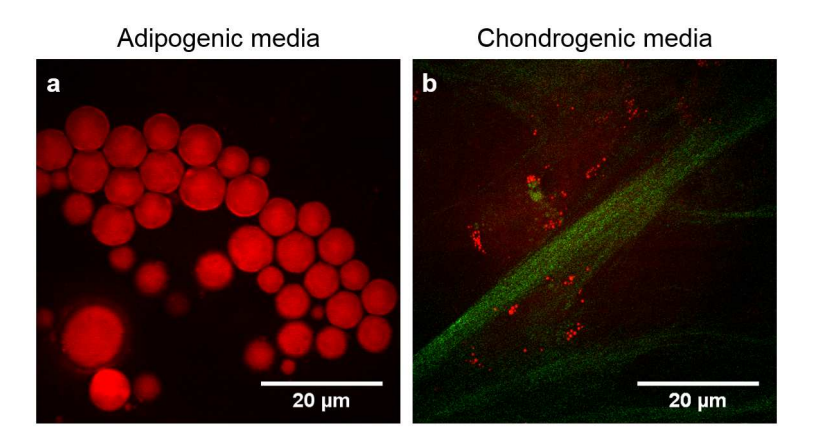


Figure 6 (a) CARS image demonstrating the formation of lipid droplets (red) in human foetal femur-derived SSCs cultured in adipogenic *in vitro* conditions; (b) multimodal imaging, using simultaneously CARS (red) and SHG (green), shows the presence of lipids and collagen fibres, respectively, in human foetal femur-derived SSCs cultured in chondrogenic media.

CARS combined with SHG and TPEF imaging has been applied by Mouras *et al.* to assessed ADSC differentiation into adipocytes and osteoblasts [64]. In the same year, Mortati *et al.* followed collagen production in living SSCs within a fibrin hydrogel scaffold in a 3D culture system using SHG and CARS [65], clearly demonstrating the potential of multimodal CARS imaging. Applications of multimodal CARS imaging in SSCs is anticipated to be an expanding field.

Most CARS imaging applications map cellular components at a single vibration frequency and do not have the same chemical selectivity as Raman spectroscopy. Broadband or hyperspectral CARS imaging overcome this limitation – the hyperspectral CARS setup provides CARS images at several vibrational frequencies and generates the corresponding spectra as in Raman spectroscopy. Di Napoli *et al.* recently reported a comparison between CARS and broadband hyperspectral CARS imaging [66]. After inducing adipogenesis in human ADSCs, CARS provided a qualitative contrast imaging while broadband hyperspectral CARS was used to determine the concentration of unsaturated lipids.

Table 3 CARS imaging applications in stem cells.

Reference (year)	Cell type	Study	Main findings
Konorov <i>et al.</i> (2007) [56]	Murine embryonic stem cells	Distinguish differentiated and undifferentiated embryonic stem cells	Preliminary images of embryonic stem cells; Need improvements in spatial resolution and image contrast
Schie <i>et al.</i> (2008) [61]	Human mesenchymal stem cells	MSC differentiation into adipocytes	Lipid droplets with high CARS contrast in 21- days differentiated adipocytes
Jo <i>et al.</i> (2011) [63]	Human adipose- derived stem cells	ADSC differentiation into adipocytes	Characterisation of ADSC differentiation into adipocytes; Lipid droplets with high CARS contrast in differentiated adipocytes
Downes <i>et al.</i> (2011) [21]	Human adipose- derived stem cells	ADSC differentiation into osteoblasts and adipocytes	Preliminary CARS imaging of differentiated osteoblasts, with frequency tuned to hydroxyapatite (960 cm ⁻¹); Lipid droplets with high CARS contrast in differentiated adipocytes
Mouras <i>at al.</i> (2012) [64]	Human adipose- derived stem cells	ADSC differentiation into osteoblasts and adipocytes	Collagen fibres detected using second harmonic generation, and osteoblasts imaged using CARS and two-photon excitation fluorescence Lipid droplets with high CARS contrast in differentiated adipocytes
Mortati <i>et al.</i> (2012) [65]	Human skeletal stem cells	Collagen production of SSCs in fibrin hydrogel scaffolds	Collagen fibres of SSCs in fibrin hydrogel scaffolds were imaged using CARS and second harmonic generation
Di Napoli <i>et al.</i> (2014) [66]	Human adipose- derived stem cells	ADSC differentiation into adipocytes	Lipid droplets with high contrast in adipocytes, comparing standard CARS and broadband hyperspectral CARS imaging; Hyperspectral CARS was more quantitative than CARS due to non-linear behaviour
Smus <i>et al.</i> (2015) [62]	Human skeletal stem cells	SSC differentiation into adipocytes	Lipid droplets with high contrast, assessed at early stages of differentiation; Modulation of human SSC differentiation using different chemical compounds assessed by CARS

Outlook

SSCs show great capacity for bone and cartilage repair and regeneration however, current techniques for SSC characterisation studies prior to cell therapeutic use are invasive and destructive. The studies discussed in this review demonstrate the potential of Raman spectroscopy and CARS imaging for enhanced characterisation of SSC differentiation in a non-invasive and non-destructive way, as neither sample preparation nor dyes/labels and other imaging contrast agents are required. We foresee the use of Raman spectroscopy and CARS imaging as standard methodologies for SSC characterisation in research studies, or even for application in regenerative medicine, evaluating and monitoring the formation of new bone/cartilage.

Raman spectroscopy has enjoyed considerable exploitation in medical diagnostics (reviewed in Kong *et al.* [67]). The translation of Raman spectroscopy from bench to clinic is currently in progress, and considerable studies are directed towards the development of optical fibre Raman probes for endoscopic applications [68]. One exciting example is the intraoperative probe created by Leblond *et al.* (using optical fibers and Raman spectroscopy) for detecting cancer cells during brain surgery [69]. Frequently, it is difficult or even impossible to distinguish cancer from non-cancer brain tissue; consequently, after surgery, malignant cells remain in the brain leading to recurrence. This probe accurately identifies invasive cancer cells in the brain, based on Raman signal, guiding the surgeon in real time in the operating room. A related development is the incorporation of a fibre optic Raman probe in a hypodermic needle, in order to achieve subcutaneous tissue measurements for *in vivo* diagnostics [70]. This non-invasive probe has huge potential for evaluating bone composition through the skin. Buckley *et al.* have applied spatially offset Raman spectroscopy, also known as SORS, to detect a compositional abnormality in the bones of a patient suffering from osteogenesis imperfecta, a genetic bone disorder that affects type I collagen [71]. The exemplar developments discussed here and others are being followed by clinical trials to validate the use of non-invasive Raman spectroscopy probes in the clinic for objective diagnostics, with the aim to improve patient outcomes and extend patient survival time.

As previously discussed in this Review, in spontaneous Raman there are few inelastically scattered photons, resulting in a weak Raman signal [29, 32, 54, 58] due to which it is used primarily for point measurements especially in clinical applications. In order to circumvent this, instruments for Raman spectroscopy systems could be improved by including more powerful detectors and advanced algorithms to enhance signal to noise. However, in CARS microscopy the Raman signal is enhanced, becoming more suitable for real-time imaging applications. For CARS imaging to be used as a routine technique several technological hurdles still need to be overcome. The majority of CARS applications were performed imaging at a single vibrational frequency, and to date only a couple of biomolecules are typically visualised using CARS microscopy (including lipids and proteins) given the limitations related to the availability of broadband laser sources. To surmount this limitation, broadband CARS techniques are being developed, where multiple Raman frequencies are imaged simultaneously [51]. It should also be mentioned that in CARS the signal is proportional to the square of the concentration of vibrational oscillators, hence for low quantities of biomolecules, CARS sensitivity considerably decreases and imaging becomes more challenging [21, 52]. Another issue is the non-resonant background observed in CARS imaging which can decrease signal to noise ratio. Potentially, these disadvantages can be addressed by using a similar coherent Raman technique named stimulated Raman scattering (SRS) (reviewed in Zhang et al. 2014 [72], and Cheng et al. 2015 [73]), though it still faces many similar challenges as CARS [73, 74]. Furthermore, CARS microscopy remains relatively expensive in comparison to other characterisation techniques, and requires sophisticated instrumentation. CARS microscopy is now commercialised by Leica Microsystems [75], but further developments are still required to make the technique more accessible. High-quality imaging systems will need to be built using affordable components, to enable and enhance uptake and application of this technique. On a different note, while Raman probes in advanced stage of translation application of CARS through optical fibres is still in its infancy. The development of special fibres that can handle laser pulses used in CARS, have large bandwidth and low distortion in the required wavelength range is an active area of research [76].

In summary while promising CARS imaging still does not provide the simplicity offered by many established characterisation techniques for skeletal regeneration for routine use. For adoption of Raman spectroscopy and CARS imaging in the clinic, in addition to overcoming the technological hurdles, it will also be necessary to: i) standardise protocols (sample preparation, data analysis and presentation, etc.), ii) perform multicentre studies, iii) provide cost rationale/justification for the national health systems, and iv) provide specific training to clinicians (reviewed in Sulé-Suso et al. [29]). Nevertheless, only by acknowledgement of the relative strengths/weaknesses and current challenges facing Raman spectroscopy and CARS imaging can a step change occur in methodologies to monitor the differentiation of SSCs in their natural state, and indeed other stem and progenitor populations in other tissues.

The research findings discussed in this review provide a strong case for the use of Raman-based techniques for skeletal stem cell characterisation. The label-free, non-destructive and non-invasive nature of Raman spectroscopy and CARS microscopy present an exciting prospective alternative to dynamically monitor SSC development for skeletal regeneration, with widespread potential in other hard and soft tissues.

Competing interests: The authors declare no competing interests.

Funding: Financial support from the Institute for Life Sciences, University of Southampton, BBSRC (BB/L021072/1), ERC grant Nano-ChemBioVision 638258 and Wessex Medical Research is gratefully acknowledged.

References:

- [1] Dawson, J.I., Kingham, E., Evans, N.R., Tayton, E. & Oreffo, R.O.C. 2012 Skeletal Regeneration: application of nanotopography and biomaterials for skeletal stem cell based bone repair. *Inflamm. Regen.* **32**, 072-089. (doi:10.2492/inflammregen.32.072).
- [2] Panteli, M., Pountos, I., Jones, E. & Giannoudis, P.V. 2015 Biological and molecular profile of fracture non-union tissue: current insights. *J. Cell. Mol. Med.* **19**, 685-713. (doi:10.1111/jcmm.12532).
- [3] Dawson, J.I., Kanczler, J., Tare, R., Kassem, M. & Oreffo, R.O.C. 2014 Concise Review: Bridging the Gap: Bone Regeneration Using Skeletal Stem Cell-Based Strategies—Where Are We Now? *Stem Cells* **32**, 35-44. (doi:10.1002/stem.1559).
- [4] Lovell-Badge, R. 2001 The future for stem cell research. Nature 414, 88-91. (doi:10.1038/35102150).
- [5] Tare, R.S., Kanczler, J., Aarvold, A., Jones, A.M., Dunlop, D.G. & Oreffo, R.O. 2010 Skeletal stem cells and bone regeneration: translational strategies from bench to clinic. *Proc. Inst. Mech. Eng. H* **224**, 1455-1470. (doi:10.1243/09544119JEIM750).
- [6] Oreffo, R.O. 2014 Centre for human development, stem cells & regeneration. *Regen. Med.* **9**, 563-567. (doi:10.2217/rme.14.48).
- [7] Srivastava, D. & Ivey, K.N. 2006 Potential of stem-cell-based therapies for heart disease. *Nature* **441**, 1097-1099. (doi:10.1038/nature04961).
- [8] Chidgey, A.P., Layton, D., Trounson, A. & Boyd, R.L. 2008 Tolerance strategies for stem-cell-based therapies. *Nature* **453**, 330-337. (doi:10.1038/nature07041).
- [9] Wickramasinghe, S.N., Porwit, A. & Erber, W.N. 2011 Chapter 2 Normal bone marrow cells: Development and cytology. In *Blood and Bone Marrow Pathology (second edition)* (eds. A. Porwit, J. McCullough & W.N. Erber), pp. 19-44. Edinburgh, Churchill Livingstone.
- [10] Bianco, P. 2014 "Mesenchymal" stem cells. *Annu. Rev. Cell Dev. Biol.* **30**, 677-704. (doi:10.1146/annurev-cellbio-100913-013132).
- [11] Bianco, P., Riminucci, M., Gronthos, S. & Robey, P.G. 2001 Bone marrow stromal stem cells: nature, biology, and potential applications. *Stem Cells* **19**, 180-192. (doi:10.1634/stemcells.19-3-180).
- [12] Bianco, P. & Robey, P.G. 2015 Skeletal stem cells. Development 142, 1023-1027. (doi:10.1242/dev.102210).
- [13] Bianco, P. & Robey, P.G. 2004 39 Skeletal Stem Cells. In *Handbook of Stem Cells* (eds. R. Lanza, J. Gearhart, B. Hogan, D. Melton, R. Pedersen, J. Thomson & M. West), pp. 415-424. Burlington, Academic Press.
- [14] Aarvold, A., Smith, J.O., Tayton, E.R., Jones, A.M., Dawson, J.I., Lanham, S., Briscoe, A., Dunlop, D.G. & Oreffo, R.O. 2014 From bench to clinic and back: skeletal stem cells and impaction bone grafting for regeneration of bone defects. *Journal of tissue engineering and regenerative medicine* **8**, 779-786. (doi:10.1002/term.1577).

- [15] Chamberlain, G., Fox, J., Ashton, B. & Middleton, J. 2007 Concise review: mesenchymal stem cells: their phenotype, differentiation capacity, immunological features, and potential for homing. *Stem Cells* **25**, 2739-2749. (doi:10.1634/stemcells.2007-0197).
- [16] Murray, I.R., West, C.C., Hardy, W.R., James, A.W., Park, T.S., Nguyen, A., Tawonsawatruk, T., Lazzari, L., Soo, C. & Peault, B. 2014 Natural history of mesenchymal stem cells, from vessel walls to culture vessels. *Cell. Mol. Life Sci.* **71**, 1353-1374. (doi:10.1007/s00018-013-1462-6).
- [17] Krause, U., Seckinger, A. & Gregory, C.A. 2011 Assays of osteogenic differentiation by cultured human mesenchymal stem cells. *Methods Mol. Biol.* **698**, 215-230. (doi:10.1007/978-1-60761-999-4_17).
- [18] Fink, T. & Zachar, V. 2011 Adipogenic differentiation of human mesenchymal stem cells. *Methods Mol. Biol.* **698**, 243-251. (doi:10.1007/978-1-60761-999-4 19).
- [19] Solchaga, L.A., Penick, K.J. & Welter, J.F. 2011 Chondrogenic differentiation of bone marrow-derived mesenchymal stem cells: tips and tricks. *Methods Mol. Biol.* **698**, 253-278. (doi:10.1007/978-1-60761-999-4 20).
- [20] Notingher, I., Jell, G., Lohbauer, U., Salih, V. & Hench, L.L. 2004 In situ non-invasive spectral discrimination between bone cell phenotypes used in tissue engineering. *J. Cell. Biochem.* **92**, 1180-1192. (doi:10.1002/jcb.20136).
- [21] Downes, A., Mouras, R., Bagnaninchi, P. & Elfick, A. 2011 Raman spectroscopy and CARS microscopy of stem cells and their derivatives. *J. Raman Spectrosc.* **42**, 1864-1870. (doi:10.1002/jrs.2975).
- [22] Robey, P.G. 2011 Cell sources for bone regeneration: the good, the bad, and the ugly (but promising). *Tissue Eng. Part B Rev.* **17**, 423-430. (doi:10.1089/ten.teb.2011.0199).
- [23] Patel, I.I., Steuwe, C., Reichelt, S. & Mahajan, S. 2013 Coherent anti-Stokes Raman scattering for label-free biomedical imaging. *J. Opt.* **15**, 094006. (doi:10.1088/2040-8978/15/9/094006).
- [24] Steuwe, C., Patel, II, Ul-Hasan, M., Schreiner, A., Boren, J., Brindle, K.M., Reichelt, S. & Mahajan, S. 2013 CARS based label-free assay for assessment of drugs by monitoring lipid droplets in tumour cells. *J. Biophotonics*. (doi:10.1002/jbio.201300110).
- [25] Lee, Y.J., Vega, S.L., Patel, P.J., Aamer, K.A., Moghe, P.V. & Cicerone, M.T. 2014 Quantitative, label-free characterization of stem cell differentiation at the single-cell level by broadband coherent anti-Stokes Raman scattering microscopy. *Tissue Eng. Part C Methods* **20**, 562-569. (doi:10.1089/ten.TEC.2013.0472).
- [26] Pijanka, J.K., Kumar, D., Dale, T., Yousef, I., Parkes, G., Untereiner, V., Yang, Y., Dumas, P., Collins, D., Manfait, M., et al. 2010 Vibrational spectroscopy differentiates between multipotent and pluripotent stem cells. *Analyst* **135**, 3126-3132. (doi:10.1039/c0an00525h).
- [27] Freudiger, C.W., Min, W., Saar, B.G., Lu, S., Holtom, G.R., He, C., Tsai, J.C., Kang, J.X. & Xie, X.S. 2008 Label-free biomedical imaging with high sensitivity by stimulated Raman scattering microscopy. *Science* **322**, 1857-1861. (doi:10.1126/science.1165758).
- [28] Schie, I.W. & Huser, T. 2013 Label-free analysis of cellular biochemistry by Raman spectroscopy and microscopy. *Compr. Physiol.* **3**, 941-956. (doi:10.1002/cphy.c120025).
- [29] Sulé-Suso, J., Forsyth, N.R., Untereiner, V. & Sockalingum, G.D. 2014 Vibrational spectroscopy in stem cell characterisation: is there a niche? *Trends Biotechnol.* **32**, 254-262. (doi:10.1016/j.tibtech.2014.03.002).

- [30] Tsai, T.H., Short, M.A., McLean, D.I., Zeng, H., McElwee, K. & Lui, H. 2014 Label-free identification and characterization of murine hair follicle stem cells located in thin tissue sections with Raman micro-spectroscopy. *Analyst* **139**, 2799-2805. (doi:10.1039/c4an00155a).
- [31] Wachsmann-Hogiu, S., Weeks, T. & Huser, T. 2009 Chemical analysis in vivo and in vitro by Raman spectroscopy—from single cells to humans. *Curr. Opin. Biotechnol.* **20**, 63-73. (doi:10.1016/j.copbio.2009.02.006).
- [32] Folick, A., Min, W. & Wang, M.C. 2011 Label-free imaging of lipid dynamics using Coherent Anti-stokes Raman Scattering (CARS) and Stimulated Raman Scattering (SRS) microscopy. *Curr. Opin. Genet. Dev.* **21**, 585-590. (doi:10.1016/j.gde.2011.09.003).
- [33] Rodriguez, L.G., Lockett, S.J. & Holtom, G.R. 2006 Coherent anti-stokes Raman scattering microscopy: a biological review. *Cytometry A* **69**, 779-791. (doi:10.1002/cyto.a.20299).
- [34] Chan, J.W. & Lieu, D.K. 2009 Label-free biochemical characterization of stem cells using vibrational spectroscopy. *J. Biophotonics* **2**, 656-668. (doi:10.1002/jbio.200910041).
- [35] Chiang, H.K., Peng, F.-Y., Hung, S.-C. & Feng, Y.-C. 2009 In situ Raman spectroscopic monitoring of hydroxyapatite as human mesenchymal stem cells differentiate into osteoblasts. *J. Raman Spectrosc.* **40**, 546-549. (doi:10.1002/jrs.2161).
- [36] Hung, P.S., Kuo, Y.C., Chen, H.G., Chiang, H.H. & Lee, O.K. 2013 Detection of osteogenic differentiation by differential mineralized matrix production in mesenchymal stromal cells by Raman spectroscopy. *PloS one* **8**, e65438. (doi:10.1371/journal.pone.0065438).
- [37] Notingher, I., Bisson, I., Bishop, A.E., Randle, W.L., Polak, J.M. & Hench, L.L. 2004 In situ spectral monitoring of mRNA translation in embryonic stem cells during differentiation in vitro. *Anal. Chem.* **76**, 3185-3193. (doi:10.1021/ac0498720).
- [38] Ichimura, T., Chiu, L.D., Fujita, K., Kawata, S., Watanabe, T.M., Yanagida, T. & Fujita, H. 2014 Visualizing cell state transition using Raman spectroscopy. *PloS one* **9**, e84478. (doi:10.1371/journal.pone.0084478).
- [39] Notingher, I., Jell, G., Notingher, P.L., Bisson, I., Tsigkou, O., Polak, J.M., Stevens, M.M. & Hench, L.L. 2005 Multivariate analysis of Raman spectra for in vitro non-invasive studies of living cells. *J. Mol. Struct.* **744–747**, 179-185. (doi:10.1016/j.molstruc.2004.12.046).
- [40] Chan, J.W., Lieu, D.K., Huser, T. & Li, R.A. 2009 Label-free separation of human embryonic stem cells and their cardiac derivatives using Raman spectroscopy. *Anal. Chem.* **81**, 1324-1331. (doi:10.1021/ac801665m).
- [41] Pascut, F.C., Kalra, S., George, V., Welch, N., Denning, C. & Notingher, I. 2013 Non-invasive label-free monitoring the cardiac differentiation of human embryonic stem cells in-vitro by Raman spectroscopy. *Biochim. Biophys. Acta* **1830**, 3517-3524. (doi:10.1016/j.bbagen.2013.01.030).
- [42] Schulze, H.G., Konorov, S.O., Caron, N.J., Piret, J.M., Blades, M.W. & Turner, R.F.B. 2010 Assessing Differentiation Status of Human Embryonic Stem Cells Noninvasively Using Raman Microspectroscopy. *Anal. Chem.* **82**, 5020-5027. (doi:10.1021/ac902697q).
- [43] Tan, Y., Konorov, S.O., Schulze, H.G., Piret, J.M., Blades, M.W. & Turner, R.F.B. 2012 Comparative study using Raman microspectroscopy reveals spectral signatures of human induced pluripotent cells more closely resemble those from human embryonic stem cells than those from differentiated cells. *Analyst* **137**, 4509-4515. (doi:10.1039/C2AN35507H).

- [44] James, S., Fox, J., Afsari, F., Lee, J., Clough, S., Knight, C., Ashmore, J., Ashton, P., Preham, O., Hoogduijn, M., et al. 2015 Multiparameter Analysis of Human Bone Marrow Stromal Cells Identifies Distinct Immunomodulatory and Differentiation-Competent Subtypes. *Stem Cell Rep.* **4**, 1004-1015. (doi:10.1016/j.stemcr.2015.05.005).
- [45] McManus, L.L., Burke, G.A., McCafferty, M.M., O'Hare, P., Modreanu, M., Boyd, A.R. & Meenan, B.J. 2011 Raman spectroscopic monitoring of the osteogenic differentiation of human mesenchymal stem cells. *Analyst* **136**, 2471-2481. (doi:10.1039/c1an15167c).
- [46] Ojansivu, M., Vanhatupa, S., Björkvik, L., Häkkänen, H., Kellomäki, M., Autio, R., Ihalainen, J.A., Hupa, L. & Miettinen, S. 2015 Bioactive glass ions as strong enhancers of osteogenic differentiation in human adipose stem cells. *Acta Biomater.* **21**, 190-203. (doi:10.1016/j.actbio.2015.04.017).
- [47] Downes, A., Mouras, R. & Elfick, A. 2009 A versatile CARS microscope for biological imaging. *J. Raman Spectrosc.* **40**, 757-762. (doi:10.1002/jrs.2249).
- [48] Mitchell, A., Ashton, L., Yang, X.B., Goodacre, R., Smith, A. & Kirkham, J. 2015 Detection of early stage changes associated with adipogenesis using Raman spectroscopy under aseptic conditions. *Cytometry A* **87**, 1012-1019. (doi:10.1002/cyto.a.22777).
- [49] Lloyd, G.R., Orr, L.E., Christie-Brown, J., McCarthy, K., Rose, S., Thomas, M. & Stone, N. 2013 Discrimination between benign, primary and secondary malignancies in lymph nodes from the head and neck utilising Raman spectroscopy and multivariate analysis. *Analyst* **138**, 3900-3908. (doi:10.1039/C2AN36579K).
- [50] Notingher, I., Bisson, I., Polak, J.M. & Hench, L.L. 2004 In situ spectroscopic study of nucleic acids in differentiating embryonic stem cells. *Vib. Spectrosc.* **35**, 199-203. (doi:10.1016/j.vibspec.2004.01.014).
- [51] Camp Jr, C.H. & Cicerone, M.T. 2015 Chemically sensitive bioimaging with coherent Raman scattering. *Nat. Photon.* **9**, 295-305. (doi:10.1038/nphoton.2015.60).
- [52] Pezacki, J.P., Blake, J.A., Danielson, D.C., Kennedy, D.C., Lyn, R.K. & Singaravelu, R. 2011 Chemical contrast for imaging living systems: molecular vibrations drive CARS microscopy. *Nat. Chem. Biol.* **7**, 137-145. (doi:10.1038/nchembio.525).
- [53] Tolles, W.M., Nibler, J.W., McDonald, J.R. & Harvey, A.B. 1977 A Review of the Theory and Application of Coherent Anti-Stokes Raman Spectroscopy (CARS). *Appl. Spectrosc.* **31**, 253-271. (doi:10.1366/000370277774463625).
- [54] Evans, C.L. & Xie, X.S. 2008 Coherent Anti-Stokes Raman Scattering Microscopy: Chemical Imaging for Biology and Medicine. *Annu. Rev. Anal. Chem.* **1**, 883-909. (doi:doi:10.1146/annurev.anchem.1.031207.112754).
- [55] Ohulchanskyy, T.Y., Pliss, A.M. & Prasad, P.N. 2011 Biophotonics: Harnessing Light for Biology and Medicine. In *Biophotonics: Spectroscopy, Imaging, Sensing, and Manipulation* (eds. D.B. Bartolo & J. Collins), pp. 3-17. Dordrecht, Springer Netherlands.
- [56] Konorov, S.O., Glover, C.H., Piret, J.M., Bryan, J., Schulze, H.G., Blades, M.W. & Turner, R.F. 2007 In situ analysis of living embryonic stem cells by coherent anti-stokes Raman microscopy. *Anal. Chem.* **79**, 7221-7225. (doi:10.1021/ac070544k).
- [57] Krafft, C., Dietzek, B. & Popp, J. 2009 Raman and CARS microspectroscopy of cells and tissues. *Analyst* **134**, 1046-1057. (doi:10.1039/B822354H).

- [58] Evans, C.L., Potma, E.O., Puoris'haag, M., Cote, D., Lin, C.P. & Xie, X.S. 2005 Chemical imaging of tissue in vivo with video-rate coherent anti-Stokes Raman scattering microscopy. *Proc. Natl. Acad. Sci. U. S. A.* **102**, 16807-16812. (doi:10.1073/pnas.0508282102).
- [59] Meyer, T., Bergner, N., Medyukhina, A., Dietzek, B., Krafft, C., Romeike, B.F.M., Reichart, R., Kalff, R. & Popp, J. 2012 Interpreting CARS images of tissue within the C–H-stretching region. *J. Biophotonics* **5**, 729-733. (doi:10.1002/jbio.201200104).
- [60] Salameh, T.S., Le, T.T., Nichols, M.B., Bauer, E., Cheng, J. & Camarillo, I.G. 2013 An ex vivo co-culture model system to evaluate stromal-epithelial interactions in breast cancer. *Int. J. Cancer* **132**, 288-296. (doi:10.1002/ijc.27672).
- [61] Schie, I.W., Weeks, T., McNerney, G.P., Fore, S., Sampson, J.K., Wachsmann-Hogiu, S., Rutledge, J.C. & Huser, T. 2008 Simultaneous forward and epi-CARS microscopy with a single detector by time-correlated single photon counting. *Opt. Express* **16**, 2168-2175. (doi:10.1364/OE.16.002168).
- [62] Smus, J.P., Moura, C.C., McMorrow, E., Tare, R., Oreffo, R.O. & Mahajan, S. 2015 Tracking adipogenic differentiation of skeletal stem cells by label-free chemically selective imaging. *Chem. Sci.* (doi:10.1039/C5SC02168E).
- [63] Jo, S.J., Choi, W.W., Lee, E.S., Lee, J.Y., Park, H.S., Moon, D.W., Eun, H.C. & Chung, J.H. 2011 Temporary increase of PPAR-gamma and transient expression of UCP-1 in stromal vascular fraction isolated human adipocyte derived stem cells during adipogenesis. *Lipids* **46**, 487-494. (doi:10.1007/s11745-011-3525-5).
- [64] Mouras, R., Bagnaninchi, P.O., Downes, A.R. & Elfick, A.P. 2012 Label-free assessment of adipose-derived stem cell differentiation using coherent anti-Stokes Raman scattering and multiphoton microscopy. *J. Biomed. Opt.* 17, 116011. (doi:10.1117/1.jbo.17.11.116011).
- [65] Mortati, L., Divieto, C. & Sassi, M.P. 2012 CARS and SHG microscopy to follow collagen production in living human corneal fibroblasts and mesenchymal stem cells in fibrin hydrogel 3D cultures. *J. Raman Spectrosc.* **43**, 675-680. (doi:10.1002/jrs.3171).
- [66] Di Napoli, C., Pope, I., Masia, F., Watson, P., Langbein, W. & Borri, P. 2014 Hyperspectral and differential CARS microscopy for quantitative chemical imaging in human adipocytes. *Biomed. Opt. Express* **5**, 1378-1390. (doi:10.1364/boe.5.001378).
- [67] Kong, K., Kendall, C., Stone, N. & Notingher, I. 2015 Raman spectroscopy for medical diagnostics From invitro biofluid assays to in-vivo cancer detection. *Adv. Drug Deliv. Rev.* **89**, 121-134. (doi:10.1016/j.addr.2015.03.009).
- [68] Bergholt, M.S., Zheng, W., Ho, K.Y., Teh, M., Yeoh, K.G., So, J.B., Shabbir, A. & Huang, Z. 2013 Fiber-optic Raman spectroscopy probes gastric carcinogenesis in vivo at endoscopy. *J. Biophotonics* **6**, 49-59. (doi:10.1002/jbio.201200138).
- [69] Jermyn, M., Mok, K., Mercier, J., Desroches, J., Pichette, J., Saint-Arnaud, K., Bernstein, L., Guiot, M.-C., Petrecca, K. & Leblond, F. 2015 Intraoperative brain cancer detection with Raman spectroscopy in humans. *Sci. Transl. Med.* **7**, 274ra219-274ra219. (doi:10.1126/scitranslmed.aaa2384).
- [70] Iping Petterson, I.E., Day, J.C., Fullwood, L.M., Gardner, B. & Stone, N. 2015 Characterisation of a fibre optic Raman probe within a hypodermic needle. *Anal. Bioanal. Chem.* **407**, 8311-8320. (doi:10.1007/s00216-015-9021-7).

- [71] Buckley, K., Kerns, J.G., Gikas, P.D., Birch, H.L., Vinton, J., Keen, R., Parker, A.W., Matousek, P. & Goodship, A.E. 2014 Measurement of abnormal bone composition in vivo using noninvasive Raman spectroscopy. *IBMS BoneKEy* 11. (doi:10.1038/bonekey.2014.97).
- [72] Zhang, D., Wang, P., Slipchenko, M.N. & Cheng, J.-X. 2014 Fast Vibrational Imaging of Single Cells and Tissues by Stimulated Raman Scattering Microscopy. *Accounts Chem. Res.* 47, 2282-2290. (doi:10.1021/ar400331q).
- [73] Cheng, J.X. & Xie, X.S. 2015 Vibrational spectroscopic imaging of living systems: An emerging platform for biology and medicine. *Science* **350**, aaa8870. (doi:10.1126/science.aaa8870).
- [74] Ozeki, Y., Umemura, W., Otsuka, Y., Satoh, S., Hashimoto, H., Sumimura, K., Nishizawa, N., Fukui, K. & Itoh, K. 2012 High-speed molecular spectral imaging of tissue with stimulated Raman scattering. *Nat. Photon.* **6**, 845-851. (doi:doi:10.1038/nphoton.2012.263).
- [75] Leica-Microsystems. 2016 CARS Microscope Label Free Imaging Leica TCS SP8 CARS. (http://www.leica-microsystems.com/products/confocal-microscopes/details/product/leica-tcs-sp8-cars/).
- [76] Latka, I., Dochow, S., Krafft, C., Dietzek, B. & Popp, J. 2013 Fiber optic probes for linear and nonlinear Raman applications Current trends and future development. *Laser Photonics Rev.* **7**, 698-731. (doi:10.1002/lpor.201200049).

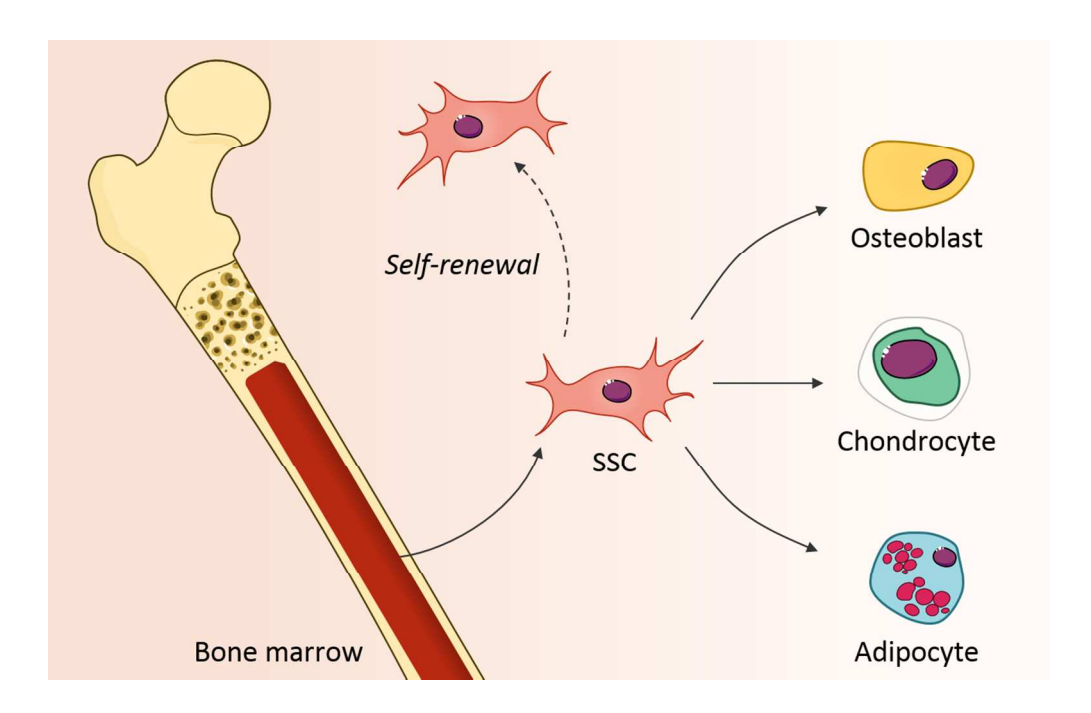


Figure 1 The differentiation potential of skeletal stem cells. A population of skeletal stem cells can be isolated and enriched from the human bone marrow, and expanded in vitro. Under appropriate conditions these skeletal stem cells have the ability to self-renew and to differentiate towards bone, cartilage and fat lineages.

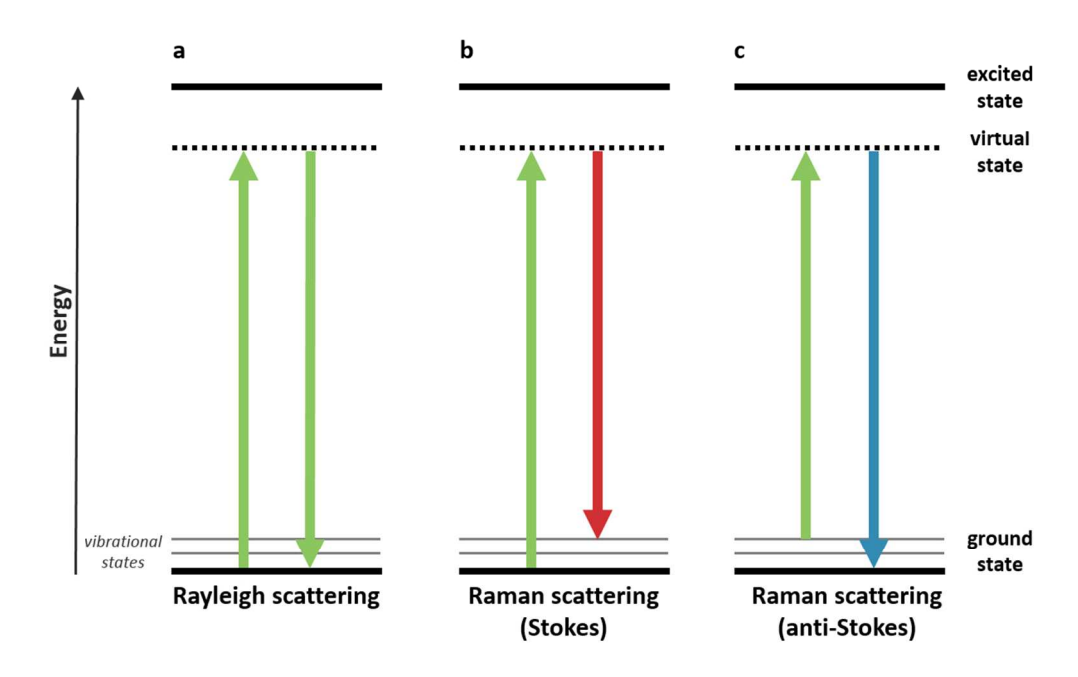


Figure 2 Schematic diagram of the energy transitions involved in Rayleigh scattering (a) and Raman scattering (b and c). Raman scattering occurs through the interaction of an incident photon with a molecular vibration mode, gaining (anti-Stokes scattering, blue-shifted) or losing (Stokes scattering, red-shifted) an amount of energy equal to that vibrational mode.

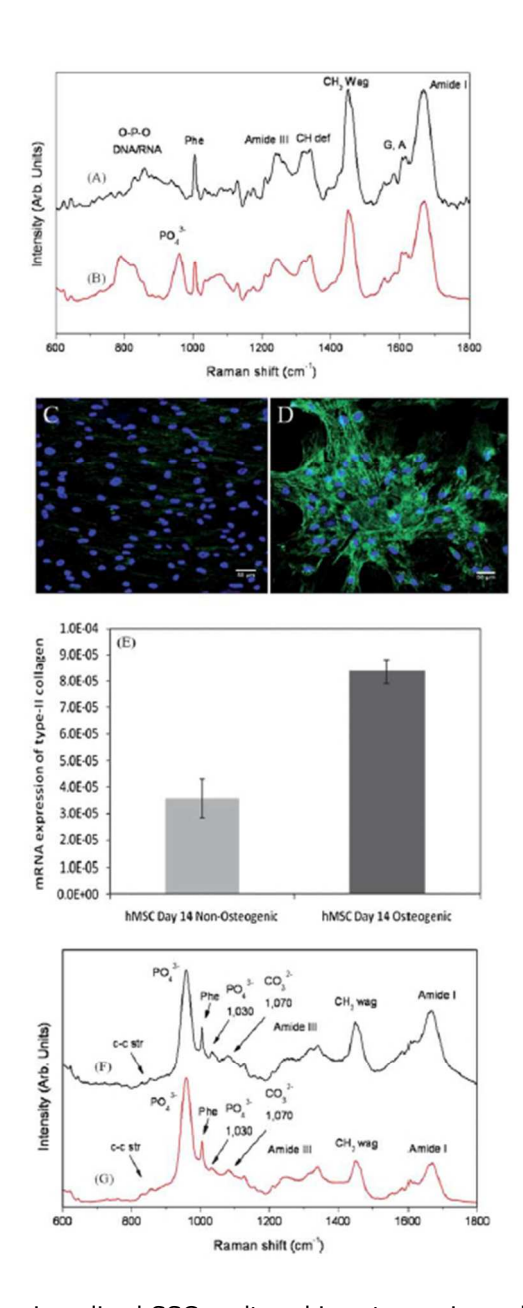


Figure 3 Raman spectra of pre-mineralised SSCs cultured in osteogenic media at day 7 (A), day 14 (B), day 21 (F) and day 28 (G). Immunocytochemical localisation of type II collagen in SSCs cultured for 14 days in basal media (C) and osteogenic media (D). Relative expression of type II collagen gene in SSCs cultured for 14 days in basal/osteogenic media, determined by qPCR (E). Adapted from [45]. Copyright Royal Society of Chemistry. Reproduced with permission.

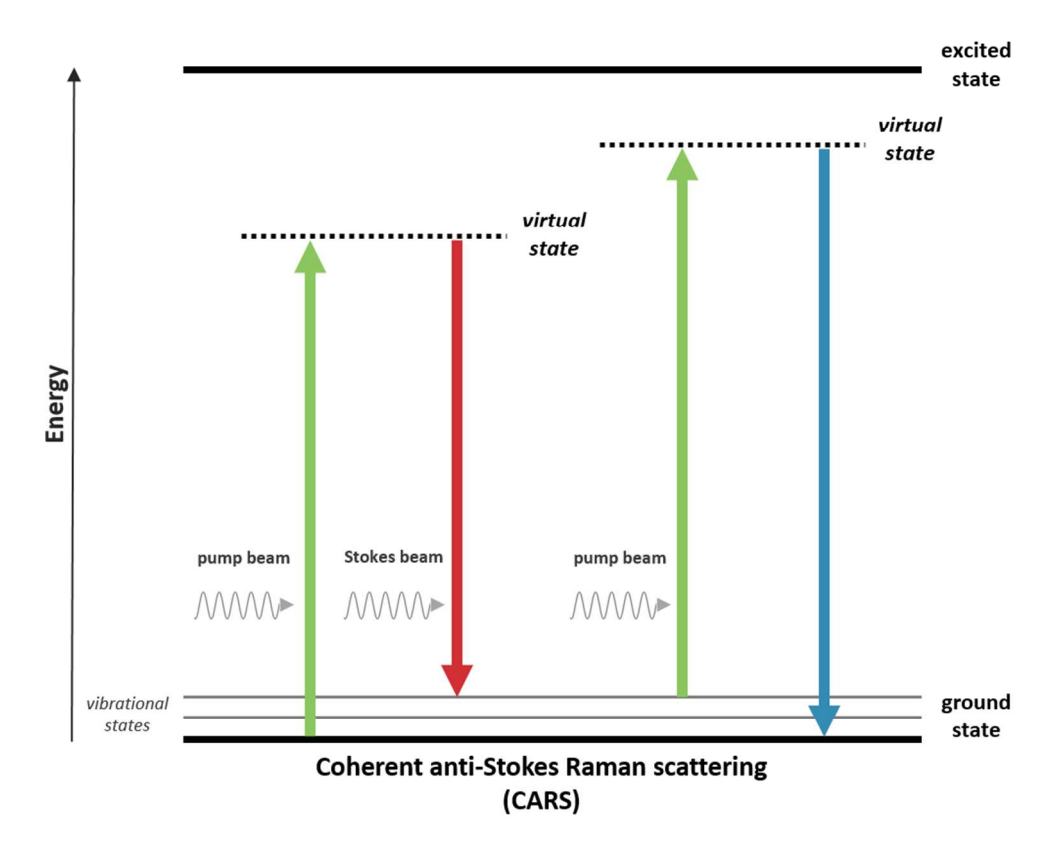


Figure 4 Schematic diagram of the energy transitions involved in coherent anti-Stokes Raman scattering (CARS). In CARS, molecular vibrational modes are coherently populated through optical pumping, by the combination of the pump and the Stokes. The vibrations coherence is probed by the pump to generate the CARS signal. Thus when the energy difference between the pump beam (higher frequency) and the Stokes beam (lower frequency) equals a particular molecular vibration of the target, the CARS signal is maximised.

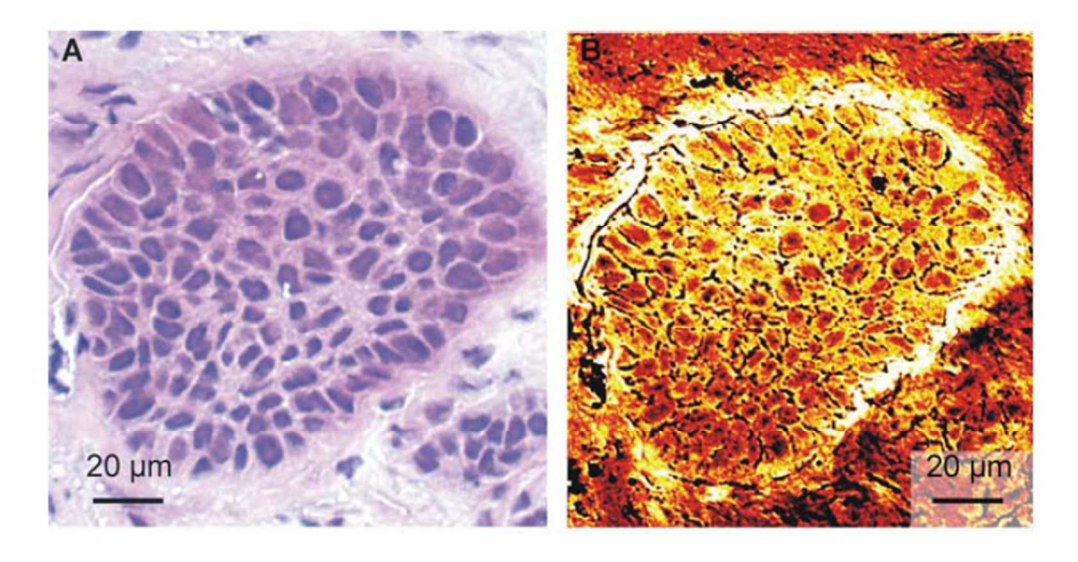


Figure 5 Comparison of H&E staining (A) and CARS imaging (B) of a human squamous-cell carcinoma metastasis in the brain. The bright components indicate the intensity of the CARS signal from lipids. Adapted from [59]. Copyright Wiley-VCH Verlag GmbH & Co. KGaA. Reproduced with permission.

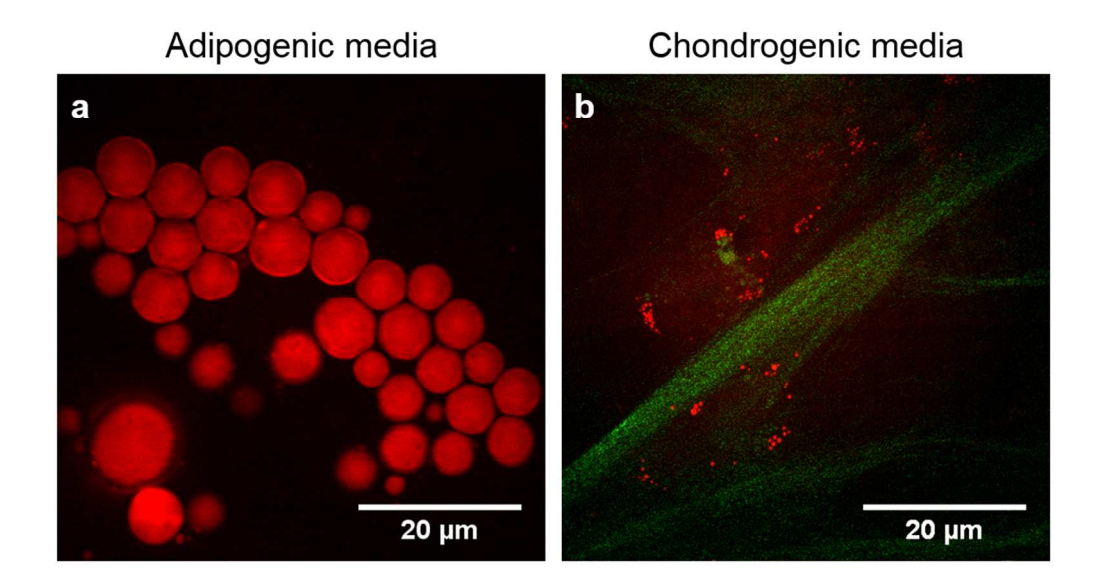


Figure 6 (a) CARS image demonstrating the formation of lipid droplets (red) in human foetal femur-derived SSCs cultured in adipogenic in vitro conditions; (b) multimodal imaging, using simultaneously CARS (red) and SHG (green), shows the presence of lipids and collagen fibres, respectively, in human foetal femur-derived SSCs cultured in chondrogenic media.